

DOHOON LEE<sup>①</sup>, TAE-YEONG SO<sup>①</sup>, HA-YOUNG YU<sup>①</sup>, GYUNSUB KIM<sup>②</sup>,  
EUSHIN MOON<sup>②</sup>, SE-HYUN KO<sup>①\*</sup>

**EFFECT OF HOT ISOSTATIC PRESSING AND SOLUTION HEAT TREATMENT  
ON THE MICROSTRUCTURE AND MECHANICAL PROPERTIES OF Ti-6Al-4V ALLOY MANUFACTURED  
BY SELECTIVE LASER MELTING**

A powder-bed-based additive manufacturing process called electron beam melting (EBM) is defined by high temperature gradients during solidification, which produces an extremely fine microstructure compared to the traditional cast material. However, porosity and segregation defects are still present on a smaller scale which may lead to a reduction in mechanical properties. It is important to have a better knowledge of the influence of post-fabrication treatments on the microstructure and mechanical characteristics before the use of additive manufacturing parts in specific applications. In this study, the effects of solution heat treatment (SHT) and hot isostatic pressing (HIP) on the microstructure and mechanical properties of Ti-6Al-4V alloy fabricated by the EBM process have been investigated. The SHT and HIP treatments can significantly improve the ductility of EBM Ti-6Al-4V due to the coarsening of  $\alpha$  laths and the formation of  $\beta$  grains.

**Keywords:** Selective laser melting; Hot isostatic pressing; Solution heat treatment; Ti-6Al-4V; Texture

## 1. Introduction

In recent years, additive manufacturing technology has advanced fast Selective laser melting (SLM), as a novel additive manufacturing (AM) technology, has great potential in modern industry [1,2]. In this technology, the parts are designed in 3D and then manufactured layer by layer as the focused laser beam scans and selectively melts the metallic powder bed [3,4]. High density, considerable material use efficiency, high design freedom, and high mechanical properties are advantages of SLM manufacturing technologies [5,6].

Due to their light weight, high strength, excellent high temperature mechanical properties, and good corrosion resistance, titanium (Ti) alloys are widely used in a variety of industries, including biomaterials and aerospace [7,8]. Ti-6Al-4V is one of the most well-known titanium alloys because of its excellent mechanical properties. Additive manufacturing of this alloy has received much interest due to its capability to manufacture near-net-shape and complex-shape parts. Specifically, to fabricate Ti-6Al-4V parts with complex shapes, SLM is one of the most attractive additive manufacturing technologies.

The melt pool is solidified at the rapid temperature gradient ( $\sim 10^{5-6}$  K/m [9]) and high cooling rate ( $\sim 10^6$  K/s [10]) in a SLM process. Such a fast cooling condition causes dynamic liquid undercooling and enhances the generation of metastable microstructures in as-built materials. It has been reported that the typical microstructure of selective laser melted (SLMed) Ti-6Al-4V alloy consists of an ultrafine non-equilibrium metastable martensite  $\alpha'$  phase and many dislocations [11]. Strong anisotropic mechanical properties are a typical characteristic of this particular microstructure, which generally leads to high yield strengths (YS) more than 1100 MPa and a serious loss of ductility (total elongation (EI) less than 10%) [12,13]. In addition, the hard and brittle structure of the fine acicular martensites  $\alpha'$  is typically attributed for the high strength and low ductility properties [14]. The SLMed Ti-6Al-4V parts require the heat treatment to enhance the mechanical properties and optimize the microstructure [15]. Post treatment, such as annealing and hot isostatic pressing (HIP), has been found to be an effective technique for controlling the microstructure and properties of the SLMed alloy.

This paper is a study on the effect of the annealing and HIP process on microstructural characteristics and mechanical prop-

<sup>1</sup> KOREA INSTITUTE OF INDUSTRIAL TECHNOLOGY (KITECH), INDUSTRIAL MATERIALS PROCESSING R&D DEPARTMENT, 156, GAETBEOL-RO, YEONSU-GU, INCHEON 406-840, REPUBLIC OF KOREA

<sup>2</sup> HUNEED TECHNOLOGIES, INCHEON, REPUBLIC OF KOREA

\* Corresponding author: shko@kitech.re.kr



erties of SLMed Ti-6Al-4V. Moreover, the mechanical properties of two built direction were also observed.

## 2. Experimental

For the SLM process, spherical plasma atomized Ti-6Al-4V powder with particle sizes ranging from 15 to 59  $\mu\text{m}$  was used. The chemical composition of the powder was 89.13Ti-6.28Al-4.16V-0.18Fe-0.20O-0.02C-0.01N-0.02H. A commercial SLM machine (M 290, EOS) was used to create specimens of Ti-6Al-4V with ASTM E8/E8M specifications. To determine the process window that could result in the fabrication of near fully dense parts, several experiments were conducted.

The optimized process parameters were as follows: a laser power of 340 W, a scanning speed of 1250 mm/s, a layer thickness of 60  $\mu\text{m}$ , a hatch spacing of 0.12 mm. To prevent the oxidation of titanium powder, argon gas is filled into the build chamber, and the process initiates when the machine sensors measure oxygen levels below 1000 ppm. The scanning strategy was performed by bidirectional scanning with a rotation of 90° between layers. In order to prevent contamination, the sample was fabricated on top of secondary supporting structures in the shape of a mesh, using the same powder composition of Ti-6Al-4V. Following the completion of the sample manufacture, the secondary supporting structures were used to make it easier to remove the samples from the build plate. Two different build orientations were used to fabricate the specimens in order to investigate the effect of build orientation on the mechanical behavior of the SLMed Ti-6Al-4V. The tensile load direction was either parallel (90°), or normal (0°) with respect to the build direction, so that the corresponding specimens will be referred to as vertical (90°) and horizontal specimens (0°). After the SLM process, annealing was conducted at 735°C for 30 min since the specimen was air-cooled, while HIP was performed at 930°C for 4 h under a 100 MPa pressure in a 99.999% Ar environment, which was followed by furnace cooling.

The tensile specimen in this research were built directly in a dog bone shape with a gage length of 24 mm, and the tensile test was performed at room temperature at a cross-head displacement rate of 3 mm/min by employing an universal testing machine (Instron 8801). The crystallographic texture was analyzed using electron backscatter diffraction (EBSD), which was carried out on a field-emission scanning electron microscope (FE-SEM, Hitachi SU-5000) equipment with an EBSD detector (Velocity Super, EDAX) at 20 keV. During the EBSD measurements, a step size of 250 nm was used for the scan area of 100  $\times$  100  $\mu\text{m}$ . Before the crystallographic analysis, all samples were sectioned parallel to the building direction. EBSD specimens were prepared by grinding with SiC paper up to 4000-grit, followed by polishing with a mixture of 90% colloidal silica (Struers OP-S).

## 3. Results and discussion

EBSD analysis was performed to further identify the phase analysis of the three specimens, as shown in Fig. 1. It was found that the all samples consists of fully hexagonal close-packed (hcp)  $\alpha/\alpha'$  phase, and the low volume fraction of  $\beta$  phase. Although the  $\alpha$  and  $\alpha'$  phases are different phases, it is difficult to identify the phases because both have the same HCP structure and lattice parameters, so it was regarded as  $\alpha/\alpha'$  in the three conditions by EBSD mapping. The cooling rate of the SLM process is extremely high, which causes the  $\beta \rightarrow \alpha'$  transformation to be dominant during cooling. The heat-treated samples can be considered as the  $\alpha$  phase because when the SLMed sample was heated to a high temperature,  $\alpha$  plates began to form at the boundary of the  $\alpha'$  needles. The acicular  $\alpha'$  of Ti alloys contains a large number of crystal defects, which can supply enough driving force for the  $\alpha' \rightarrow \alpha + \beta$  transformation when the sample is appropriately heat-treated [15]. The volume fraction of  $\beta$  phase increases after annealing, it is indicated that the  $\alpha'$  phase decomposed into  $\alpha$  and  $\beta$  phase. However, after the HIP treatment, the

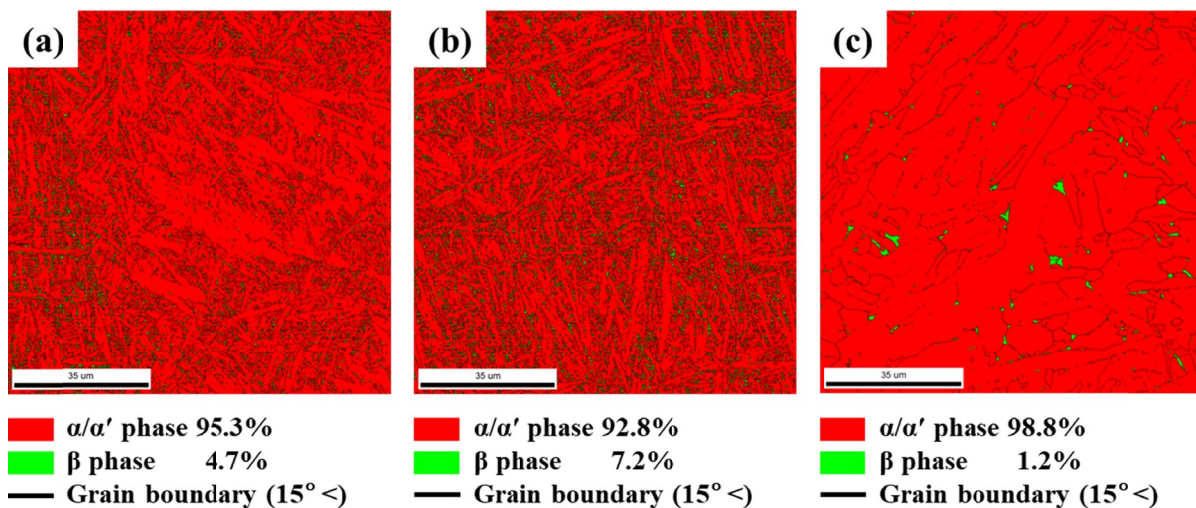


Fig. 1. EBSD observations exhibit the distribution of grain boundaries and phase maps of SLMed Ti-6Al-4V alloy after different heat treatments including (a) SL Med, (b) annealing and (c) HIP

volume fraction of  $\beta$  phase decreases, and it seems that  $\alpha'$  to  $\alpha$  transformation was more active than  $\alpha'$  to  $\beta$ .

Fig. 2 presents the image quality (IQ), inverse pole figure (IPF) maps and grain size distribution of EBSD results in the Ti-6Al-4V samples followed by SLMed, annealing and HIP treatment. The IPF map of the SLMed sample indicated that the prior- $\beta$  grain boundary has elongated along the building direction, and the columnar structures on both sides of the prior- $\beta$  grain boundary show completely different orientations. The grain size of the samples is about 3.5  $\mu\text{m}$ , 3.8  $\mu\text{m}$  and 10.9  $\mu\text{m}$  in the SLMed, annealing and HIP, respectively. The metastable  $\alpha'$  phase transforms into the stable  $\alpha$  phase after annealing, while the morphology and size of  $\alpha$  phase are still similar to the  $\alpha'$  phase. It indicated that the newly generated  $\alpha$  phases not only replace the prior  $\alpha'$  phases but also tend to preserve the original morphology of the prior  $\alpha'$  phase during annealing process. However, the grain size is significantly larger in the sample after the HIP treatment at 930°C, which contributed to the coarsening and spherizing of  $\alpha$  and  $\beta$  phases.

Fig. 3 shows the kernel average misorientation (KAM) maps to analyze the local strain distribution in samples with different deformation gradients. High KAM values indicate higher plastic deformation or dislocation accumulation along high-angle grain boundaries. Due to the characteristics of the SLM process with a fast cooling rate, the SLMed sample exhibits a high KAM degree as a result of the formation of  $\alpha'$  phase and a high dislocation density. Heat treatment is required to remove residual stresses since this microstructure could have high strength but low ductility. Fig. 3(b,c) shows that the average KAM degree is lower after annealing and HIP treatment, and it indicates that the residual stress is relieved as the heat treatment temperature increases.

Fig. 4 shows ultimate tensile strengths (UTS), yield strengths (YS), and elongations (EL) of the vertically (90°) and horizontally (0°) fabricated SLMed Ti-6Al-4V after different heat treatments. The UTS and YS decreased while the EL increased after HIP treatment, indicating that HIP treatment reduced fracture toughness but increased the plasticity of SLMed

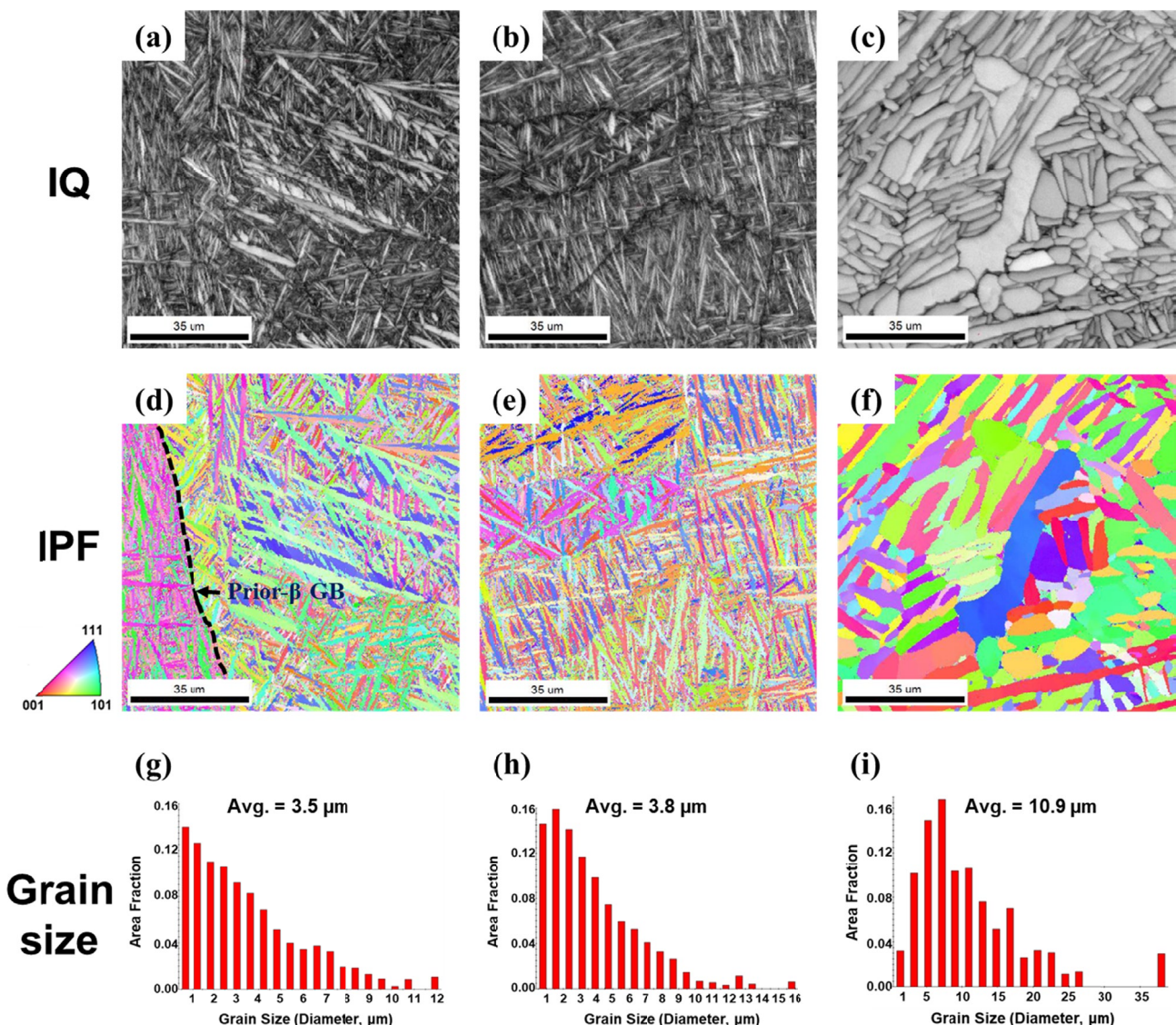


Fig. 2. EBSD observations exhibiting with IQ, IPF maps and grain size distribution of SLMed Ti-6Al-4V alloy after different heat treatments including (a, d, g) SLMed, (b, e, h) annealing and (c, f, i) HIP

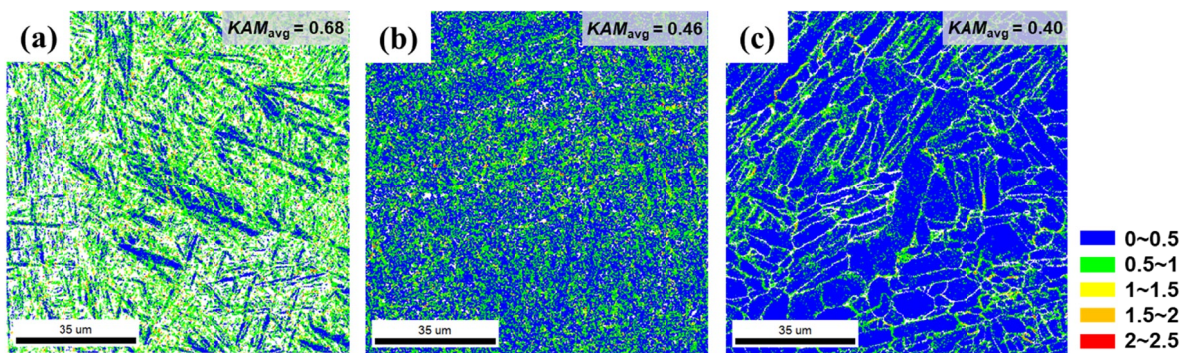


Fig. 3. EBSD KAM maps of SLMed Ti-6Al-4V alloy after different heat treatments including (a) SLMed, (b) annealing and (c) HIP

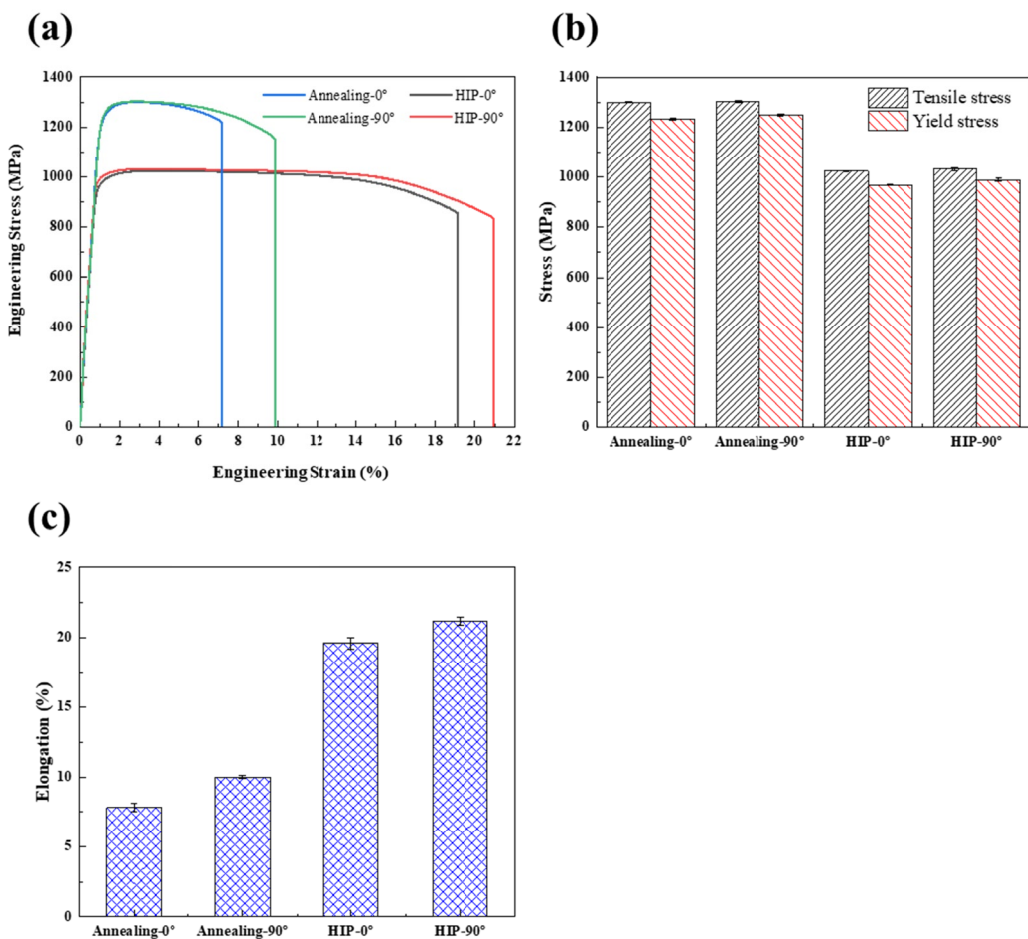


Fig. 4. Tensile properties of the annealing and HIP samples with different building direction (a) Engineering stress-strain curves, (b) Summary of the UTS, YS, (c) Summary of the Elongation

Ti-6Al-4V. This was mainly related to the fine and acicular  $\alpha$  phase in the annealing sample. According to Hall-Petch theory, the microstructure of fine grain has a large number of grain boundaries, resulting in more resistance to dislocation motion, which is positive for enhancing the strength but harmful to the plasticity. However, coarsening and spherizing of  $\alpha$  phase in the HIP treated sample contributes to enhancing the plasticity, while decreases the strength.

Under the same heat treatment condition, the strength is similar, while the elongation is different along the building direction. The anisotropy in mechanical properties is considered to be

caused by defects in the SLM manufacturing process because this sample does not exhibit any strong texture. The HIP treated sample shows less elongation anisotropy than the annealing sample, which indicates that the HIP treatment is able to reduce the defect and alleviate the mechanical anisotropy of SLMed Ti-6Al-4V.

#### 4. Conclusions

This work study on the influence of post-heat treatments on microstructure and mechanical properties of the selective laser

melting processed Ti-6Al-4V titanium alloy. The main conclusions are summarized as follows:

- 1) Due to the high cooling rate in SLM technology, SLMed Ti-6Al-4V shows a columnar prior- $\beta$  grain boundary microstructure with acicular  $\alpha'$  martensite phase filled inside. After the annealing at 735°C, the metastable  $\alpha'$  phase was transformed into the  $\alpha$  and  $\beta$  phases, and the volume fraction of  $\beta$  phase increased, while the morphology was similar to that of the SLMed microstructure. After the HIP treatment at 930°C, the  $\alpha$  and  $\beta$  phases morphology changed to coarsening and spherizing, and grain size significantly increased.
- 2) The KAM map shows that the average KAM degree is lower after the heat treatment, and the residual stress is relieved as the heat treatment temperature increases, which results in enhanced ductility.
- 3) The strength was increased due to the fine  $\alpha$  phase after annealing, while the grain size was coarsened after the HIP treatment, which results in higher ductility. In addition, HIP treatment induces compressive stress on the material, reducing internal porosity and removing aligned prior  $\beta$  grain boundaries along the building direction, while promoting grain growth of the  $\alpha$  phase, resulting in reduced defects and mechanical anisotropy.

#### Acknowledgments

This work was supported by the Korea Institute of Industrial Technology (Project number IR220057).

#### REFERENCES

- [1] H. Shipley, D. McDonnell, M. Culleton, R. Coull, R. Lupoi, G. O'Donnell, D. Trimble, Optimization of process parameters to address fundamental challenges during selective laser melting of Ti-6Al-4V: a review. *Int. J. Mach. Tool. Manuf.* **128**, 1-20 (2018).
- [2] Q.Q. Han, R. Setchi, S.L. Evans, Synthesis and characterisation of advanced ball-milled Al-Al<sub>2</sub>O<sub>3</sub> nanocomposites for selective laser melting. *Powder Technol.* **297**, 183-192 (2016).
- [3] K.J. Lin, L.H. Yuan, D.D. Gu, Influence of laser parameters and complex structural features on the bio-inspired complex thin-wall structures fabricated by selective laser melting. *J. Mater. Process. Tech.* **267**, 34-43 (2019).
- [4] D. Wang, W.H. Dou, Y.Q. Yang, Research on selective laser melting of Ti6Al4V: surface morphologies, optimized processing zone, and ductility improvement mechanism. *Metals* **8**, 471 (2018).
- [5] B.B. He, W.H. Wu, L. Zhang, L. Lu, Q.Y. Yang, Q.L. Long, K. Chang, Microstructural characteristic and mechanical property of Ti6Al4V alloy fabricated by selective laser melting. *Vacuum* **150**, 79-83 (2018).
- [6] H. Tekdir, A.F. Yetim, Additive manufacturing of multiple layered materials (Ti6Al4V/316L) and improving their tribological properties with glow discharge surface modification. *Vacuum* **184**, 109893 (2021).
- [7] G. Lütjering, J.C. Williams, *Titanium*, (2nd ed.), Springer, Berlin pp. 15-50 (2007).
- [8] G. Wang, Z. Chen, J. Li, J. Liu, Q. Wang, R. Yang, Microstructure and Mechanical Properties of Electron Beam Welded Titanium Alloy Ti-6246. *J. Mater. Sci. Technol.* **34**, 570-576 (2018).
- [9] X. He, G. Yu, J. Mazumder, Temperature and composition profile during double-track laser cladding of H13 tool steel. *J. Phys. D Appl. Phys.* **43** (2010), Article 015502.
- [10] C. Qiu, M.A. Kindi, A.S. Aladawi, et al., A comprehensive study on microstructure and tensile behaviour of a selectively laser melted stainless steel. *Sci. Rep.* **8**, 7785 (2018).
- [11] J. Yang, H. Yu, J. Yin, M. Gao, Z. Wang, X. Zeng, Formation and control of martensite in Ti-6Al-4V alloy produced by selective laser melting. *Mater. Des.* **108**, 308-318 (2016).
- [12] P. Kumar, O. Prakash, U. Ramamurty, Micro-and meso-structures and their influence on mechanical properties of selectively laser melted Ti-6Al-4V. *Acta Mater.* **154**, 246-260 (2018).
- [13] L. Thijs, F. Verhaeghe, T. Craeghs, J. Van Humbeeck, J.P. Kruth, A study of the microstructural evolution during selective laser melting of Ti-6Al-4V. *Acta Mater.* **58**, 3303-3312 (2010).
- [14] T. Voisin, N.P. Calta, S.A. Khairallah, J.-B. Forien, L. Balogh, R.W. Cunningham, A.D. Rollett, Y.M. Wang, Defects-dictated tensile properties of selective laser melted Ti-6Al-4V. *Mater. Des.* **158**, 113-126 (2018).
- [15] Dong-Hoon Yang, Young-Kyun Kim, Yujin Hwang, Myoung-Se Kim, Kee-Ahn Lee, Effect of Dry-Electropolishing on the High Cycle Fatigue Properties of Ti-6Al-4V Alloy Manufactured by Selective Laser Melting. *J. Korean Powder Metall. Inst.* **26**, 471-476 (2019).